

See discussions, stats, and author profiles for this publication at: <https://www.researchgate.net/publication/233786903>

Prony Series Spectra of Structural Relaxation in N-BK7 for Finite Element Modeling

ARTICLE in THE JOURNAL OF PHYSICAL CHEMISTRY A · NOVEMBER 2012

Impact Factor: 2.69 · DOI: 10.1021/jp307717q · Source: PubMed

CITATIONS

3

READS

96

5 AUTHORS, INCLUDING:



[Erick Koontz](#)

Clemson University

11 PUBLICATIONS 11 CITATIONS

SEE PROFILE



[Peter Wachtel](#)

IRradiance Glass

26 PUBLICATIONS 81 CITATIONS

SEE PROFILE



[J. David Musgraves](#)

IRradiance Glass

82 PUBLICATIONS 440 CITATIONS

SEE PROFILE



[Kathleen Richardson](#)

University of Central Florida

285 PUBLICATIONS 3,721 CITATIONS

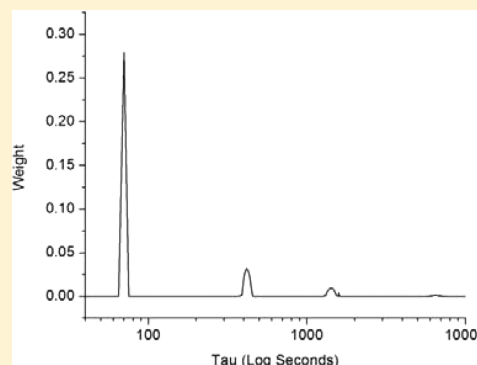
SEE PROFILE

Prony Series Spectra of Structural Relaxation in N-BK7 for Finite Element Modeling

Erick Koontz,* Vincent Blouin, Peter Wachtel, J. David Musgraves, and Kathleen Richardson

Department of Material Science and Engineering, Clemson University, Clemson, South Carolina 29634, United States

ABSTRACT: Structural relaxation behavior of N-BK7 glass was characterized at temperatures 20 °C above and below T_{12} for this glass, using a thermal mechanical analyzer (TMA). T_{12} is a characteristic temperature corresponding to a viscosity of 10^{12} Pa·s. The glass was subject to quick temperature down-jumps preceded and followed by long isothermal holds. The exponential-like decay of the sample height was recorded and fitted using a unique Prony series method. The result of this method was a plot of the fit parameters revealing the presence of four distinct peaks or distributions of relaxation times. The number of relaxation times decreased as final test temperature was increased. The relaxation times did not shift significantly with changing temperature; however, the Prony weight terms varied essentially linearly with temperature. It was also found that the structural relaxation behavior of the glass trended toward single exponential behavior at temperatures above the testing range. The result of the analysis was a temperature-dependent Prony series model that can be used in finite element modeling of glass behavior in processes such as precision glass molding (PGM).



1. INTRODUCTION

Structural relaxation is the movement of a glassy material's atomic structure toward its equilibrium structure under a given temperature condition.¹ The structural relaxation behavior of various oxide glasses^{2–4} has been studied in the past to understand the physics behind relaxation and to better predict glass behavior with respect to temperature. Developing coherent models for structural relaxation in all glasses has been a goal of researchers for many years.

The Kohlrausch function is often used to describe processes that are not purely exponential.

$$\phi(t) = \exp\left[-(t/\tau)^\beta\right] \quad (1)$$

Another model that is widely used in the characterization of stress relaxation in glasses is the Generalized Maxwell model in which the relaxation of stress in a glass is represented by a Prony series.¹

$$\phi(t) = \sum_{i=1}^N w_i e^{-\left(\frac{t}{\tau_i}\right)} \quad (2)$$

This model was used by Duffrène et al. to study shear stress relaxation behavior of soda-lime-silicate glass via creep testing as well as other glass types.⁵ The Prony series has also been extended to characterization of stress relaxation behavior for precision molding of glass optics.⁶

In order to obtain an accurate finite element model (FEM) to describe the response of a material, the properties of that material must be well characterized. For the modeling of the precision glass molding (PGM) process, the characterization of structural relaxation behavior is expected to not only lead to

better final shape predictions for a molded optic but also provide insight into properties that depend on the optic's thermal history. Structural relaxation has no standard characterization method or expression, though enthalpy relaxation curves measured by differential scanning calorimetry (DSC) are often used in conjunction with the Tool–Narayanaswamy–Moynihan model.⁴ However, it is necessary to choose the most appropriate method for the FEM of precision glass molding. Direct measurements of structural relaxation can be done using a thermal mechanical analyzer (TMA), where the measurement method will be as close, in form, to precision glass molding as possible.

The following is an adaptation of the Prony series for the characterization of structural relaxation as measured via TMA. The technique employs a modified fitting method for use in the FEM of the thermo-mechanical behavior of N-BK7, which is a well understood optical glass.^{3,6} The fitting method used in this research is an extension and modification of the collocation method described by Tschoegl and originally laid out by Schapery in his doctoral dissertation.^{7,8} The original collocation method involves choosing the time constants (τ_i) and solves for the weights (w_i). The method used below uses a unique process for identifying which time constants to select for the final curve fit. It was inspired by a similar method also developed by Tschoegl in which the idea of strictly defined windows of time is used to reduce the error of a least-squares approach to fitting experimental data.^{9–13}

Received: August 3, 2012

Revised: November 26, 2012

Published: November 27, 2012



2. EXPERIMENTAL SECTION

The samples used in this experiment were 3 mm × 3 mm bars of Schott N-BK7 with a height between 15 and 17.5 mm and polished, parallel end faces.

The structural relaxation behavior of these samples was analyzed using a TA Instruments Thermomechanical Analyzer (TMA 2940). The samples were tested vertically as demonstrated in Figure 1. Thin platinum foil was placed

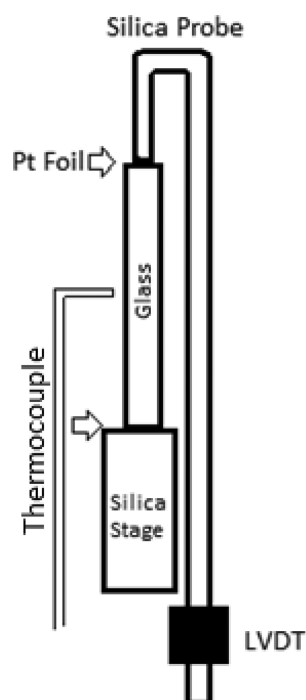


Figure 1. TMA schematic.

between the sample and the instrument's fused quartz stage as well as between the sample and the fused quartz probe to prevent interdiffusion at the elevated temperatures tested here. The instrument's K-type thermocouple was positioned at half the sample height and as close to the sample as possible without touching it. The furnace was carefully lowered and the initial height measurement taken using the TMA probe.

The first series of measurements consisted of 10 °C temperature down-jumps followed by isothermal holds. The lengths of the isothermal holds were determined by previous experiments in which it was determined how long it took for complete structural relaxation to occur. Relaxation was determined to be complete when the change in length versus time became a constant linear value. In the case of the 20 °C ΔT , the isothermal hold before the temperature step was approximately 5.5 h long and the hold after the temperature step was just over 9 h. A representative schematic of the temperature profile is provided in Figure 2. These measurements were performed for final test temperatures spaced every 5 °C from 542 °C. This final test temperature is 15 °C below T_{12} (557 °C), and the experiment included steps up to 577 °C. T_{12} is the temperature that corresponds to a viscosity of 12 log (Pa*s). Tests conducted at starting temperatures below T_{12} included a 5 °C/min ramp to 562 °C to reset the thermal history of the sample, followed by a 1 °C/min ramp down to the starting test temperature.^{1,14} Runs to temperatures above T_{12} did not require this initial step as the thermal history of the

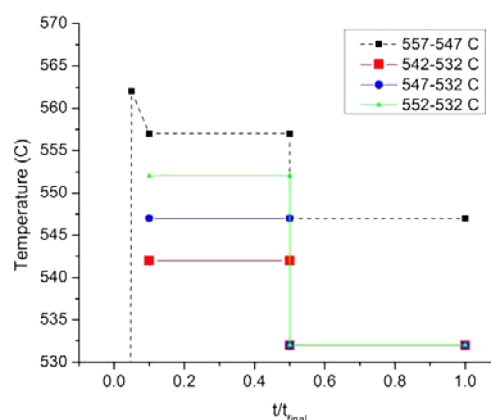


Figure 2. Experimental schedule: temperature versus normalized time for a 10 °C down-jump (dashed line) and for varying temperature down-jumps (solid lines).

piece is rewritten at $T > T_{12}$. An appropriate isothermal hold time was determined for each test temperature by measuring the time it took for the change in sample height to reach a constant slope. This constant slope is a result of the steady state deformation of the sample under the force of the probe; its linear nature signifies the absence of exponential-like structural relaxation.

Once an isothermal hold was complete at the starting test temperature, a 10 °C jump down was initiated at a rate of 20 °C/min. The final temperature was then held isothermally until the sample reached structural equilibrium. The data sampling period was set at 40 s/point during the preliminary stages and changed to 0.5 s/point for the first several hundred seconds after a temperature step was initiated, then reverted back to the original sampling period. A maintenance force of 0.05 N was exerted by the probe at all times in order to maintain contact with the sample while influencing the resultant structural relaxation behavior as little as possible. The probe force is essentially the same as the force from the weight of the sample; since the tests were carried out below the softening point of the glass, no nonlinear deflection occurred. The probe force was exerted on the sample at all times during both isothermal holds and the test itself. At a given temperature, this deflection is linear and constant. The sample was fabricated to stand upright, and no buckling occurred during the tests.

In addition to the 10 °C temperature down-jump experiments, a series of tests were carried out in which the down-jump (ΔT) was varied from 10 to 20 °C. The final temperature for all of these runs was the same, 532 °C, as shown in Figure 2. This evaluation was performed to assess the effect of the starting temperature versus final temperature on the Prony spectrum. The varying ΔT runs followed the same procedure as the constant ΔT runs listed above.

3. DATA ANALYSIS

3.1. Data Conditioning. Structural relaxation is the configurational aspect of an amorphous material's response to a change in temperature environment. Changes in thermodynamic properties of the glass such as enthalpy and molar volume lag behind the change in ambient temperature as shown in Figure 3. The fictive temperature (T_f) is used to state at what temperature the glass's existing structure and properties would be in equilibrium.¹⁵

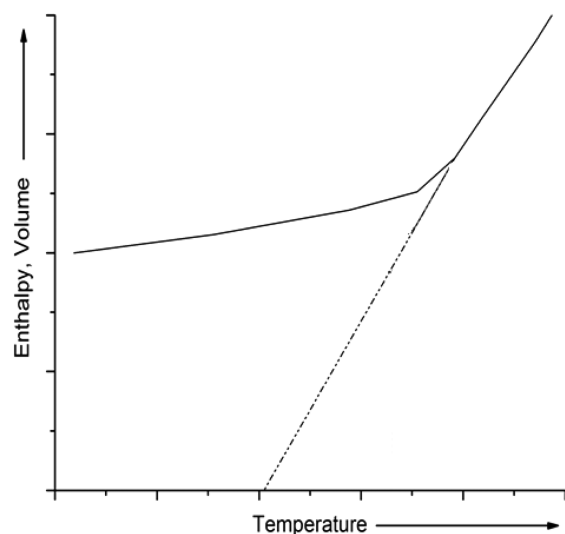


Figure 3. Volume/enthalpy versus temperature for a generic glassy material.

For this reason, glasses that are quenched from above T_g to below T_g more quickly will have a higher fictive temperature because the equilibrium structure corresponding to a higher temperature liquid is frozen upon cooling. When a glass is subjected to an ambient temperature different than its T_f , which is high enough that the constituents in the glass are free to move, it will structurally rearrange, gradually changing its T_f to the temperature to which it is exposed. It is this configurational aspect of the material structure and its change with temperature that is of interest. The raw data collected by TMA contains not only the structural relaxation due to configuration change but also an instantaneous thermal expansion response and time-dependent viscous flow response. The viscous flow response is due to the sample slowly deforming under its own weight as well as the contribution from the probe maintenance force, which is approximately equivalent to the sample weight. The steady-state sample deflection occurred on the order of $0.1 \mu\text{m/h}$. These effects must be removed in order to study the structural relaxation behavior, a graphical description is provided in Figure 4.

To extract the purely configurational component of the observed relaxation in the present study, the data was first

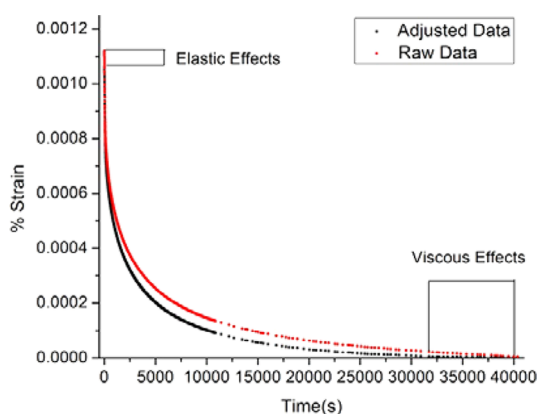


Figure 4. Comparison of raw configurational expansion data to data adjusted to remove steady-state viscous flow of the material as well as instantaneous expansion.

adjusted by removing the material's instantaneous (elastic) response to the temperature jump, which is dictated by the thermal expansion coefficient of the glass, referred to as α_g . In order to remove this elastic response, keeping in mind that the furnace temperature does not change instantaneously, the total elastic deflection due to temperature change was calculated using eq 3

$$\Delta L_{\text{elastic}} = \alpha_g L \Delta T \quad (3)$$

where ΔT is the magnitude of the temperature down-jump, $\Delta L_{\text{elastic}}$ is the elastic component of the length change, and L is the original sample length. Having combined the result of this equation with the effective ramp rate (R), determined as the rate at which the sample reached the target temperature, which was $\sim 10^\circ\text{C/min}$, eq 4 was obtained, where $\Delta L_{\text{elastic}}(t)$ is the elastic change in length as a function of time. This was applied from $t = 0$ min to the time at which the target temperature was reached in the sample.

$$\Delta L_{\text{elastic}}(t) = \frac{\Delta L_{\text{elastic}}}{\left(\frac{\Delta T}{R}\right)} t \quad (4)$$

Having compensated for the elastic component of the mechanical response to temperature, the next step in the data reduction is the removal of the viscous flow component of the material's response. This was accomplished by identifying the long-time section of the data that exhibits a constant slope. Two points were selected at the beginning of the constant slope section, and their midpoint on the curve was found. Likewise, the same operation was performed near the end of the data. This resulted in two points on the curve. Between these points, a line was drawn and the slope calculated. The slope was then multiplied by the time vector so that the curve was effectively adjusted by rotating about time = 0. This slope adjustment function was added to the data curve and effectively removed the viscous component of the material's mechanical response to temperature change.

3.2. Curve Fitting. Analysis of the adjusted relaxation data was performed by fitting the data using a Prony series (eq 2), which is well-suited and widely used for fitting and analyzing many kinds of relaxation data.^{16–19} Fitting of the experimental data was done using Matlab's optimization function, FMINCON, and a least-squares approach to minimize the error between the experimental data and the fitting function. The method of fitting and the requisite number of parameters required for fitting were also of interest in this study. The extensive setup of the fitting process is described below.

The Prony parameters of interest as seen in eq 2 are w_i , the weight coefficient, and τ_i , the tau or time constant. The data, adjusted as described above, is fitted with a Prony series given the following conditions: (1) the sum of the weights, w_i , is constrained to unity, and (2) the tau values, τ_i , are specified and input to the curve fitting solver, therefore leaving the solver the freedom to solve for the weight terms only. An example of the original data and resulting fit can be seen in Figure 5. Note, the TMA used cannot achieve a high enough sampling rate to accurately sample short time experimental data (i.e., $t < 50$ s); therefore, the fit is preferential to longer times. Because of the fact that 4 orders of magnitude are being sampled during the entirety of the test, it was decided to sacrifice the very short time fit for the sake of fitting the majority of the data well.

The collocation method mentioned in the introduction is an ancestor to the method employed for finding the fit parameters.

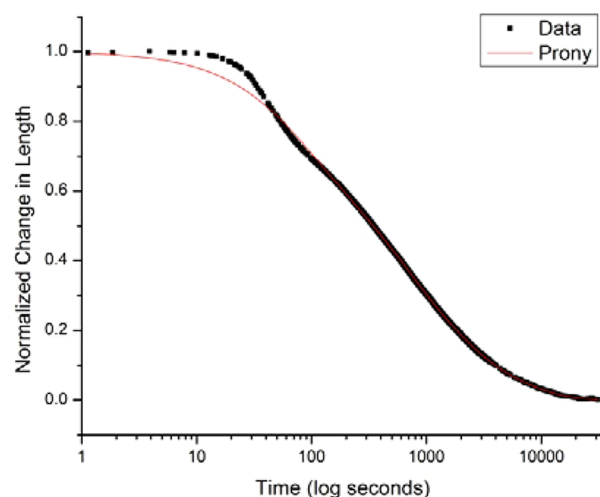


Figure 5. Normalized experimental data plotted against a full term Prony fitting function.

The method employed here differs from the collocation method in that, rather than picking select taus to serve as a basis for the fit, hundreds and thousands of taus are input to the solver in an attempt to discern which are significantly weighted.

The manner in which the tau values are input in this analysis is unique to the method: an array of taus is input by incrementing the values from $\tau_i \approx 0$ (zero cannot be used for numerical reasons) to $\tau_N = t_{\text{final}}$ in increments of time (i.e., 100, 50, 10, and 1 s). Where t_{final} is the length of the test in seconds. This results in the input matrix being filled with a large number of potential values. The aim is to provide the solver with many reasonable time constants and allow the solver to determine which of the time constants will have significantly nonzero weights and then use the significant taus found by the solver to refit the data in search of accurate weights.

To confirm that the conditions described were rigid enough to allow the solver to converge while flexible enough to freely describe the curve, several tests were done. In the first test used to test the accuracy of the optimization process, a test function was constructed from a predefined Prony series and that test function was fit by the program as described above. The weight and tau values estimated by the curve fitting routine were exactly those of the predefined Prony series. This confirmed the assumption that the Prony terms found by the solver are able to accurately describe a given set of data. Second, to ensure that the solver did not settle in a local minimum of the parameter space based on the order in which the tau values were fed to the optimizer, the input tau array was randomized. Here, the resulting curve fit was shown to match the curve fit of the nonrandomized input array validating that the order of tau inputs does not affect the solution produced by the solver.

Having ensured that the curve fit could be trusted; the experimental data was fitted using the following method. The first fitting of each curve was performed with what will be referred to as a tau step size of 100 s ($\tau = [\sim 0, 100 \text{ s}, 200 \text{ s}, 300 \text{ s}, 400 \text{ s}, \dots, t_{\text{final}}]$). The result of interest is a plot of the weights, w_i , versus the taus, τ_i for the Prony series in eq 2. A representative plot of a 50 s step size, of which Figure 6 is an example, will be referred to as a Prony spectrum.

The most easily distinguished feature of the spectrum is the appearance of four definite peaks corresponding to four distributions of significantly weighted tau values; the majority

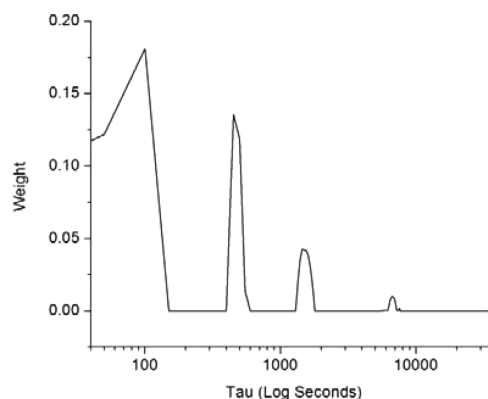


Figure 6. Prony series spectrum: weight terms versus tau terms for temperature jump from 552 to 542 °C; step size, 50 s.

of the τ_i values had an associated w_i value of zero. The test duration, t_{final} , from the initial temperature down-jump to the attainment of full structural equilibrium, was on the order of 10^4 seconds, meaning that the number of tau terms input to the solver for that length of time is typically greater than 100. If using smaller step sizes, the number of terms can reach as high as 15 000. The fact that the majority of the taus input were not significantly weighted reinforces the validity of this curve fitting method. Out of a possible 15 000 tau values, only four relatively narrow groups have significant weights, and these four pairs of weight and tau parameters match the data curve well. Allowing the solver to weight any of those thousands of tau inputs with any combination of weights, provided they sum to unity, and obtaining four definitive tau peaks with significantly nonzero weights leads to the conclusion that the parameters found are a description of the curve and not a random artifact of the solver.

The next operation was to reduce the step size of the input tau to a number on the order of 50 s ($\tau = [\sim 0, 50 \text{ s}, 100 \text{ s}, 150 \text{ s}, 200 \text{ s}, \dots, t_{\text{final}}]$) and refit the curve. This produced a spectrum with narrower, more well-defined peaks and tau values similar to those calculated using the larger step size. This suggests that, as the input step size decreases, the accuracy of the solver to find the tau peaks increases. Once this step was completed, a new tau array was constructed using a step size of 5 s. The step size was refined only around the peak locations to lessen the fitting time. This was confirmed to be a valid approach by fitting an entire set of data with a 5 s step size and comparing it to the set with a refined fit only around the peaks. As can be seen in Figure 7, the spectrum resulting from the smaller step size fit had more clearly defined peaks than both the 50 and 100 s fittings.

The 5 s step size Prony fit was determined to be the best step size for determining the tau values, as a balance between optimizer computing time and fitting accuracy. The R^2 for the fit shown in Figure 7, with several thousand terms, was 0.9996241. In addition, each Prony spectrum peak contained multiple tau values, indicating that each peak consists of a distribution of taus. Relaxation behavior in most glasses is known to be nonexponential in nature; the presence of a distribution indicates that this holds true for structural relaxation.²⁰ The use of step sizes smaller than 5 s did not produce notably different maximum peak tau values or peak widths. In order to test whether or not, as the four peaks suggest, the experimental data could be most accurately represented with at least a four-term Prony series, the max tau values from each peak were selected and input back into the

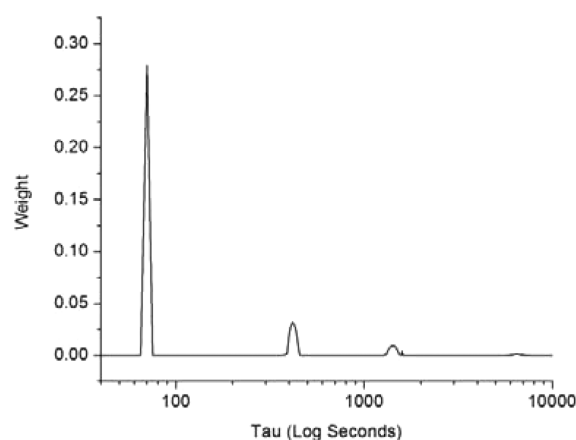


Figure 7. Prony series spectrum for temperature jump from 552 to 542 °C; step size, 5 s.

solver as the tau array. The curve was fitted again using the four selected taus. The resulting curve was compared to the original data to quantify the fitting accuracy. The R^2 for the fit with four terms was 0.9996239. Figure 8 confirms that the resulting four-

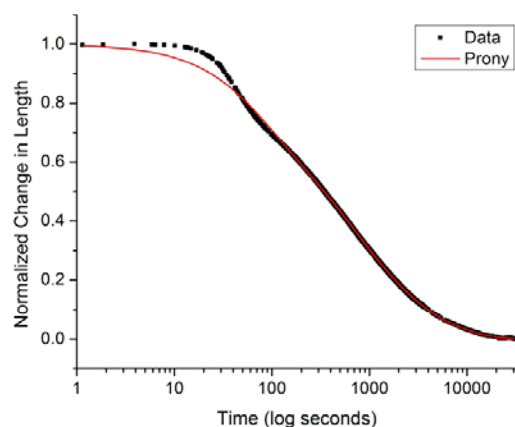


Figure 8. Normalized experimental data plotted with a four-term Prony series fitting function.

term fit was essentially as good as the fit that included several thousand Prony terms. The natural conclusion is to assume that, in this glass and at this temperature and ΔT condition, four terms are the minimum number of terms that should be used to describe the configurational aspect of structural relaxation. This smaller number of terms also makes utilizing this method reasonable for defining structural relaxation parameters in a way that could be used in finite element modeling.

To test the assertion that four terms are indeed the minimum necessary to fit the curve, an analysis was done in which the maximum tau values from each peak were fed to the solver; however, only three of the four tau values was used. The term to be left out was alternated. In this way, several three-term series were tested. The fit of the data with a three-term series was less accurate and a visibly poorer fit. Of the three-term fits, the best was the exclusion of the second relaxation time. A summary of the R^2 values is shown in Table 1. Various other approaches including averaging two adjacent tau values and inputting them were used and proved to be significantly less accurate than the four-term fit.

Table 1. R^2 Values for Curve Fits Using Different Numbers of Prony Terms

# of Prony terms	R^2
>15 000	0.9996241
4	0.9996239
3	0.98792 ^a

^aThis fit was the best of all 3-term combinations tried.

In light of the accuracy of this method to determine how many peaks and what tau values should be used to best describe the data, the next step was to fit each set of data with the tau values indicated by the 5 s step size spectrum. This approach used the fewest number of tau values possible (four) and therefore should have produced the most accurate weights available for a small number of terms. All tau values came from the 5 s step size spectra, and all weight values came from the subsequent fit with only those aforementioned tau values. These pairs of tau and weight values accurately and uniquely model the experimental data.

The data gathered from the experiments detailed in the experimental section were analyzed using the procedure described above. Although the measurements were done to obtain change in sample height, this change in height can be directly related to the fictive temperature of the glass using eq 5.

$$\frac{dh}{h_i} = \alpha_g dT + (\alpha_l - \alpha_g) dT_f \quad (5)$$

where h is the sample height, h_i is the initial sample height, T_f is the fictive temperature, and $\alpha_l - \alpha_g$ is the liquid thermal expansion coefficient minus the thermal expansion coefficient of the glass. The subtraction of the glass thermal expansion from the liquid thermal expansion defines what is known as the configurational expansion, which is the expansion directly related time-dependent rearrangement of the glass network during structural relaxation.

Using eq 5, the experimental data and the model derived from it can be used to express how the fictive temperature of the glass changes with time and temperature.

4. RESULTS

4.1. Varying Temperature Jumps. Tests done with varying magnitudes of temperature change (ΔT) displayed an interesting result. Figure 9 shows that, although the temperature jumps ranged from 10 to 20 °C, the tau values did not vary significantly and, in fact, are almost identical using the width of a given peak from a 5 s tau step size as the error of the peak tau value. This would seem to show that, since all of the jumps were to a common temperature, the final temperature dictates the Prony tau peak position rather than the magnitude of the jump. It remains to be seen if extreme temperature jumps such as 50 or 100 °C bear out the same trend. In the present case, much more time is spent at the final temperature than the starting temperature over the course of the fictive temperature relaxation, so this result should not be surprising.

The relaxation curves of the different temperature jumps are visibly different; therefore, if the tau parameters are similar between them, one can then assume the weight parameters must be the distinguishing factor. Table 2 shows the parameters. The weights for shorter time tau values are higher for larger temperature jumps, whereas the weights for longer time taus are higher for smaller temperature jumps.

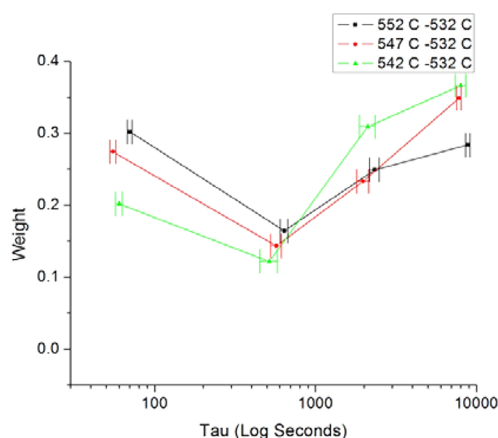


Figure 9. Final Prony spectra for 20, 15, and 10 °C temperature jumps.

Table 2. Final Prony Tau and Weight Values for 20, 15, and 10 °C Temperature Jumps

	552–532 (°C)	547–532 (°C)	542–532 (°C)
τ_1	70.1	55.1	60.1
w_1	0.30219	0.27446	0.20209
τ_2	640.1	570.1	515.1
w_2	0.16445	0.14363	0.12191
τ_3	2330	1970	2110
w_3	0.24929	0.23326	0.30939
τ_4	8860	7785	7985
w_4	0.28408	0.34866	0.3666

The weights indicate what percentage or share of the total relaxation is described by the corresponding tau-dependent exponential term. Thus, it stands to reason that runs with a lower starting viscosity and higher driving force for structural relaxation (ΔT) see more dominant short time relaxation. In contrast, runs from temperatures at which the glass is not as free to move and does not have as much pressure on it to do so, complete a greater percentage of their relaxation over longer times. This is confirmed and well described by the trends seen in Figure 9.

4.2. Constant Temperature Jumps. Figure 10 shows a comparison of the eight fitted relaxation curves used in this study. All R^2 values were at least 0.99; most were at least 0.999. The physical relaxation trend is as expected, with the higher temperature, lower viscosity samples relaxing quicker than the

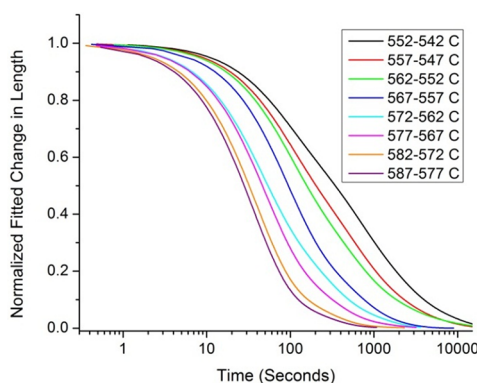


Figure 10. Prony fit curves of TMA structural relaxation data from 542 to 577 °C.

high viscosity samples. Figure 11 shows the resulting Prony series parameters as determined by the method described in section 3.

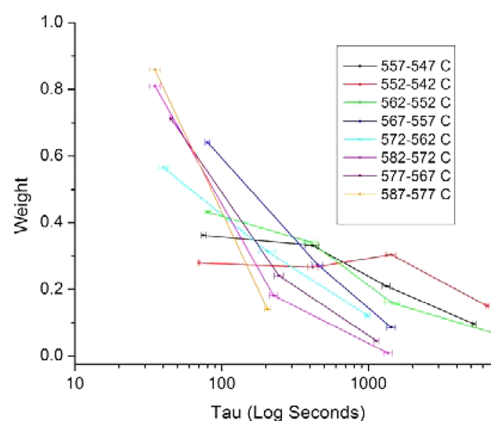


Figure 11. Prony series final spectra for 10 °C down-jumps from 547 to 577 °C.

An interesting point in Figure 11 is that the tau values of each distinct peak do not vary strongly with temperature, and when error bars are added, most peaks from adjacent temperatures are statistically the same. The error is calculated as the tau peak widths from the 5 s step size spectrum. However, with an increase in temperature, there is a notable occurrence: the longest tau peak disappears from the spectra. Between the 552 °C case and the 557 °C case, the longest time peak disappears, leaving only three peaks, and in a similar way, between the 572 °C case and the 577 °C case, both the third and fourth peaks disappear. As the temperature increases, the longest time tau peak in a spectrum decreases in weight until it reaches zero. Decreasing viscosity will give rise to a faster, short-time relaxation and the importance of the longest characteristic relaxation time will decrease until it ceases to describe the relaxation behavior and therefore ceases to exist or is too small to be observed.

Characterizing the observed trend in Prony weights may give some insight into the atomic scale nature of the structural relaxation behavior of the glass and provide means for better characterization of relaxation behavior for use in FEM of precision glass molding. Figure 12 is a plot of the weight of

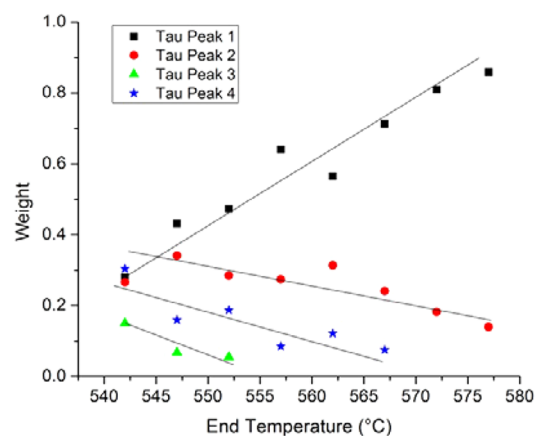


Figure 12. Tau peak weighting vs temperature for 10 °C temperature down-jumps from 547 to 577 °C.

each Prony spectrum peak with respect to temperature. The weight trend is fairly linear in all cases. The first peak weights are continually increasing, while all peaks corresponding to longer relaxation times are continually decreasing as a function of increasing temperature. This trend indicates, as would be expected, that with increasing temperature, the behavior of the configurational aspect of the material's mechanical response to temperature change is moving toward a single exponential expression.

4.3. Application to FEM. The goal of the present work has been to characterize the structural relaxation of N-BK7 glass using eq 2 in such a way as to maximize its utility in FEM applications. This end goal implies the need for a description of the structural relaxation as a function of temperature and time; so that the FEM models can be used to accurately describe processes such as the deformation of molded optical elements upon cooling.

The initial result of this study was the appearance of a finite and repeatable number of characteristic peaks. This occurrence answers a fundamental question, which is how many Prony terms are needed to describe the structural relaxation behavior of this glass. The results shown in the previous section indicate that the characteristic time scales of relaxation (τ_i) are essentially unchanged with temperature, whereas the weights assigned to each of these time scales in the Prony expression vary linearly with temperature, as shown in Figure 12. The weight trends for structural relaxation behavior of N-BK7 can be described by a simple linear fit detailed in Table 3.

Table 3. Weight Linear Fit Parameters

	slope (m)	intercept (b)	R^2
peak 1	0.0157	−8.1739	0.94
peak 2	−0.0042	2.6196	0.6
peak 3	−0.0084	4.826	0.85
peak 4	−0.0095	5.29	0.85

With the weights expressed as functions of temperature and the approximation that the tau values are essentially static in this temperature range, the structural relaxation can be represented as a function of temperature within the considered temperature range.

$$\frac{dh}{h_i} = \sum_{i=1}^4 (m_i T + b_i) \exp\left[-t/\tau_i\right] \quad (6)$$

Equation 6 defines the essentially linear displacement induced by structural changes in the glass. However, this model is only a preliminary expression of the structural relaxation model of N-BK7. In the current form, the model is somewhat limited in accuracy to temperature jumps of ~ 10 °C. This equation can be input to a FEM by specifying a temperature and time-dependent thermal expansion property and be used to predict the structural relaxation induced shape change of N-BK7 within the model's range of operation.

5. DISCUSSION

For the varying temperature down-jump relaxations with a common final temperature at 532 °C, seen in Figure 2, no significant shift in tau peaks was observed with changing ΔT . This was originally thought to be a result of the common ending temperature. The glass sample is at the final fictive temperature for the majority of the relaxation event; therefore,

it would make sense that the tau peaks were similar for different ΔT values given that they reflected the relaxation time constants at 532 °C. The corresponding weight terms showed trends that relate to the difference in ΔT values. Cases with higher ΔT resulted in more strongly weighted short time relaxation due to the lower starting viscosity and larger driving force to reach structural equilibrium. Conversely, cases with lower ΔT showed more significantly weighted longer relaxation times. This is due to a smaller initial driving force for structural relaxation and a higher starting viscosity.

Originally, the lack of tau dependence on ΔT was thought to be caused by the common final temperature of those runs; however, upon investigation of fixed 10 °C jump cases, a similar phenomenon was observed. Figure 11 shows that, for final temperatures from 547 – 577 °C, the peak tau values are essentially the same, given the error bars on the data. This was unexpected but supports the finding from the varying ΔT case that, for this glass at least, the relaxation time constants are not sensitive to temperature within the range tested. The interesting aspect of the fixed 10 °C jump cases is the trends in the weight terms, shown in Figure 12.

The weight for each maximum tau value changes linearly with final temperature. Only the first peak shows a continual increase in weight, while all other peaks decrease with increasing temperature. This trend is confirmed by the fact that, as the temperature is increased within the experiment, the longest time peak eventually disappears from the spectrum all together. For instance, at 542 °C, there are four significantly weighted tau peaks, while at the top of the tested temperature range (577 °C), only 2 peaks remain visible in the spectrum. Although the temperature tested was not high enough to observe the disappearance of the second peak, the weight functions experimentally derived predict that only the first peak will remain at high temperature. This would describe a super cooled liquid that exhibits a single relaxation time.²¹ Characterization of structural relaxation in a form useful for input into FEM will allow this glass to be accurately modeled through the glass transition range. At high temperatures, glass behavior trends toward single exponential relaxation behavior, while at lower temperatures, glasses behave like solids. The range between amorphous solid and super cooled liquid has been the focus of this article.

6. CONCLUSION

Structural relaxation measurements were carried out on N-BK7 using a TMA. Measurements were taken by stepping down in temperature after an isothermal hold and allowing the glass to relax to structural equilibrium. Temperatures from 542 to 577 °C (spaced every 5 °C) were tested using 10 °C down-jumps. A series of experiments were also performed where temperature steps were made from 542, 547, and 552 °C down to 532 °C.

The data was fit in Matlab with a Prony series using a unique parameter input method developed specifically for this analysis, and Prony fitting parameters (w_i , τ_i) were analyzed. The analysis showed that this material exhibited multiple relaxation times at each temperature condition and that the relaxation times did not vary significantly with temperature. The weights, however, showed an essentially linear variation with temperature. The first tau peak increased in weight with increasing temperature, while the other tau peaks continually decreased in weight with increasing temperature, meaning the material trended toward single exponential relaxation behavior at higher temperatures.

A linear fit was applied to the weights as a function of temperature, and the resulting linear equations were inserted into eq 2. The resulting eq 6 characterizes the structural relaxation behavior of N-BK7 from 542 to 577 °C in 10 °C increments and can be input into a FEM for limited predictive modeling of precision glass molding. A modification of the FEM thermal expansion input to include the time-dependent expansion defined in eq 6 would be sufficient to account for structural relaxation in a FEM. Work is being done on the completion of the structural model for N-BK7 utilizing trends in Prony weights and time constants with respect to different temperature jumps. The characterization of these trends along with the work presented here will provide a full picture of the structural relaxation behavior of N-BK7 in the temperature range where kinetic rearrangement of the glass structure is possible.

AUTHOR INFORMATION

Notes

The authors declare no competing financial interest.

ACKNOWLEDGMENTS

We would like to thank the Army Research Office for support (ARO 56858-MS-DPS). We thank Dr. Paul Joseph and also Dr. Ulrich Fotheringham and Scott Gaylord for their insights.

REFERENCES

- (1) Varshneya, A. K. *Fundamentals of Inorganic Glasses*; Academic Press: New York, 2006.
- (2) Rekhson, S. M. *J. Non-Cryst. Solids* **1985**, *73*, 151–164.
- (3) Gaylord, S.; Ananthasayanam, B.; Tincher, B.; Petit, L.; Cox, C.; Fotheringham, U.; Joseph, P.; Richardson, K. *J. Am. Ceram. Soc.* **2010**, *93*, 2207–2214.
- (4) Moynihan, C. T.; Crichton, S. N.; Opalka, S. M. *J. Non-Cryst. Solids* **1991**, *131*, 420–434.
- (5) Kadali, H. C. *Experimental Characterization of Stress Relaxation in Glass*. Ph.D. Thesis, Clemson University, 2009.
- (6) Ananthasayanam, B. *Computational Modeling of Precision Molding of Aspheric Glass Optics*. Ph.D. Thesis, Clemson University, 2008.
- (7) Tschoegl, N. W. Representation by Series-Parallel Models. In *The Phenomenological Theory of Linear Viscoelastic Behavior: An Introduction*; Springer-Verlag: Berlin, Germany, 1989; pp 136–145.
- (8) Schapery, R. A. *Irreversible Thermodynamics and Variational Principles with Applications to Viscoelasticity*. Ph.D. Thesis, California Institute of Technology, 1962.
- (9) Emri, I.; Tschoegl, N. W. *Proc. Int. Congr. Rheol.* **1992**, 910–910.
- (10) Tschoegl, N. W.; Emri, I. *Rheol. Acta* **1993**, *32*, 322–7.
- (11) Emri, I.; Tschoegl, N. W. *Rheol. Acta* **1993**, *32*, 311–21.
- (12) Emri, I.; Tschoegl, N. W. *Rheol. Acta* **1994**, *33*, 60–70.
- (13) Emri, I.; Tschoegl, N. W. *Int. J. Polym. Mater.* **1998**, *40*, 55–79.
- (14) Schott AG. *Optical Glass Catalogue*, 2007, 10.
- (15) Shelby, J. E. In *Introduction to Glass Science and Technology*; The Royal Society of Chemistry: Cambridge, UK, 2005.
- (16) Fuchs, M.; Gotze, W.; Hofacker, I.; Latz, A. *J. Phys.: Condens. Matter* **1991**, *3*, 5047–71.
- (17) Slanik, M. L.; Nemes, J. A.; Potvin, M.; Piedboeuf, J. *Mech. Time-Depend. Mater.* **2000**, *4*, 211–230.
- (18) Ghoreishy, M. H. R. *Mater. Des.* **2012**, *35*, 791–797.
- (19) Duffrene, L.; Gy, R.; Burlet, H.; Piques, R. *J. Rheol.* **1997**, *41*, 1021–38.
- (20) Scherer, G. W. *J. Non-Cryst. Solids* **1990**, *123*, 75–89.
- (21) Brawer, S. A. *J. Chem. Phys.* **1984**, *81*, 954–75.